Space–Time Variability of Rainfall and Extreme Flood Response in the Menomonee River Basin, Wisconsin

YU ZHANG AND JAMES A. SMITH

Department of Civil and Environmental Engineering, Princeton University, Princeton, New Jersey

(Manuscript received 26 December 2001, in final form 5 October 2002)

ABSTRACT

The hydrometeorological processes that control flash flooding are examined through analyses of space–time rainfall variability and flood response in the Milwaukee metropolitan region. The analyses focus on four flood events in the Menomonee River basin that occurred 21 June 1997, 2 July 1997, 6 August 1998, and 21 July 1999. The June 1997 and August 1998 flood events produced record flood peaks in the Menomonee River and its tributaries. Rainfall analyses, which are based on WSR-88D radar reflectivity observations and rainfall measurements from a dense network of rain gauges maintained by the city of Milwaukee, provide rainfall fields for each event at 1-km spatial resolution and 5-min timescale. The June 1997 and August 1998 storms exhibited striking contrasts in storm structure, evolution, and motion. Analyses of the structure and evolution of these storms are presented in conjunction with scaling analyses of the rainfall fields. The contrasting storm-scale properties of the June 1997 and August 1998 events resulted in sharp contrasts in extreme flood response between the two events. The regional flood response of the Menomonee River basin is examined in terms of space–time rainfall variability and heterogeneous land surface properties. Analyses are based on radar rainfall fields and 15-min discharge observations from stream gauging stations, with drainage area ranging from 47 to 319 km^2 for the four flood events. Extreme flood response is examined in terms of flood peak magnitudes, peak response times, and event water balance. A distributed hydrologic model, which includes a Hortonian infiltration model and a network-based representation of hillslope and channel response, plays a central role in examining the regional flood response.

1. Introduction

The Menomonee River, which drains much of the Milwaukee metropolitan region (Fig. 1), experienced record flooding 21 June 1997 and 6 August 1998. Sample flood frequency distributions (Fig. 2) for the Menomonee River at Wauwautosa [319 km^2; U.S. Geological Survey (USGS) gauge number 04087120] and its tributaries Underwood Creek (47 km^2; USGS gauge number 04087088) and the Menomonee River at Menomonee Falls (90 km^2; USGS gauge number 04087030) illustrate the magnitudes of flood peaks for the two events and the contrasting flood response between the urbanized lower basin (Underwood Creek) and the agricultural upper basin (Menomonee River above Menomonee Falls).

The hydrograph of the Menomonee River at Wauwautosa for the 21 June 1997 flood (Fig. 3) exhibited three peaks in response to multiple pulses of heavy rainfall over the basin. The form of flood response in the Menomonee River basin is tied to both storm properties and land surface properties. In this paper, we examine the hydrometeorological processes that control extreme flood response in the Menomonee River basin. The 21 June 1997 and 6 August 1998 events in the Menomonee River basin provide the principal targets of opportunity for study of space–time variability of rainfall and extreme flood response. Analyses of flood events on 2 July 1997 and 21 July 1999 are used to further examine flood response properties of the Menomonee River basin.

Our approach to extreme flood analysis is by necessity event-based and opportunistic as opposed to driven by observations from carefully designed field campaigns in experimental watersheds. Extreme, flood-producing storms are spatially and temporally rare and are seldom represented in the observations from experimental watersheds. In this study, our experimental base consists of two contrasting storms that produced record floods within the 319 km^2 Menomonee River basin (21 June 1997 and 6 August 1998), a short-duration, extreme rainfall rate storm (2 July 1997) that is used to examine the ''unit response'' of the Menomonee River basin, and a storm (21 July 1999) consisting of multiple pulses of heavy rainfall, like the 21 June 1997 storm, but with somewhat smaller storm total accumulation than the 21 June 1997 storm.

Corresponding author address: Dr. James A. Smith, Dept. of Civil and Environmental Engineering, Princeton University, Princeton, NJ 08544.
E-mail: jsmith@princeton.edu

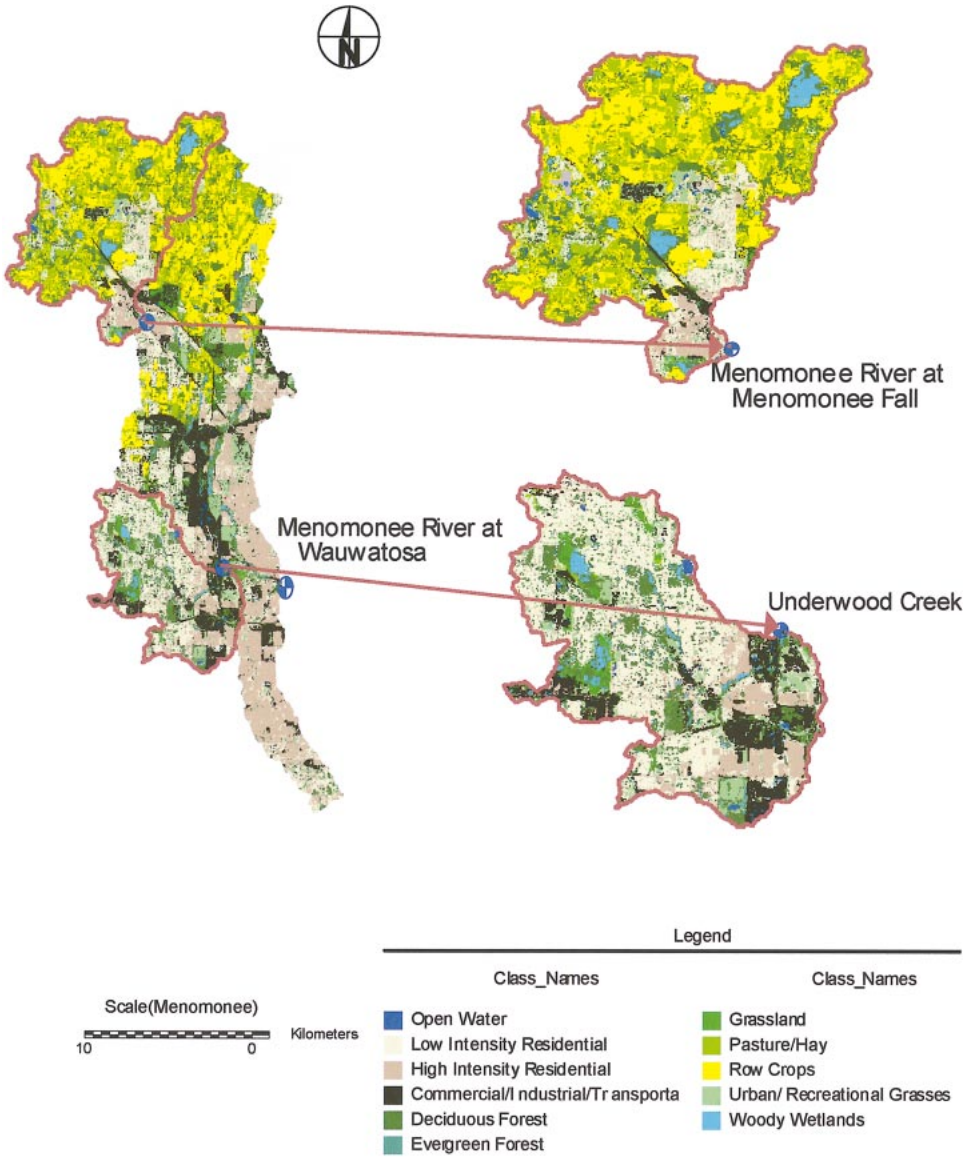

FIG. 1. Land use and land cover (LULC) for the Menomonee River basin. Blowups of the Underwood Creek basin and Menomonee Falls basin are included. Stream gauging stations are denoted by blue-shaded circles.

Extreme flood response in the Menomonee River basin is examined in terms of flood peak magnitudes, peak response times, and event water balance for the four flood events. Discharge observations at 15-min timescale from the three stream gauging stations (see Figs. 1–3) and radar rainfall fields with 1-km horizontal scale and 5-min timescale are used for diagnostic and hydrologic model analyses of peak response and event water balance. The distributed hydrologic model used in this study (see Morrison and Smith 2001; and Giannoni et al. 2003) consists of a Hortonian infiltration model (the Green–Ampt model with moisture redistribution; see Ogden and Saghafian 1997) and a network-based hillslope and channel response model (see also Rodriguez-Iturbe and Rinaldo 1997; Vieux and Bedient 1998).

The Menomonee River basin has a wide range of land use and land cover properties (Fig. 1), resulting in a heterogeneous mix of hydrologic response properties. The basin consists of wetlands, agricultural land, impervious regions distributed throughout the urban portions of the basin, and residential regions, some with and some without detention basins. Storm sewers are found throughout the nonagricultural areas of the basin. Our knowledge of hydrologic response is strongest in homogeneous drainage basins, yet many of the scientific, engineering, and resource management problems concerning flood response are focused on heterogeneous catchments with land surface properties that are changing over time (see, e.g., Potter 1991). Urbanizing regions are especially important in terms of engineering

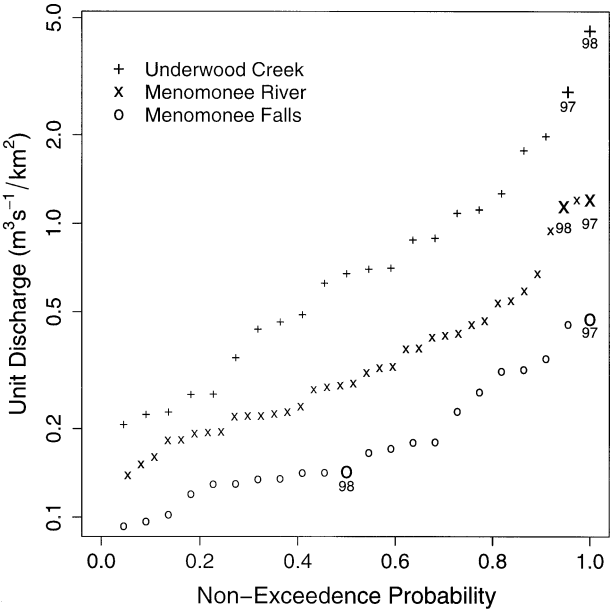

FIG. 2. Quantile plots of annual flood peaks for Menomonee River at Menomonee Falls (USGS ID: 04087030; 25-yr record), Menomonee River at Wauwatosa (USGS ID: 04087120; 39-yr record) and Underwood Creek (USGS ID: 04087088; 22-yr record). Flood peaks on 21 Jun 1997 and 6 Aug 1998 are highlighted 97 and 98, respectively. Peak discharge is represented as a unit discharge ($m^3\ s^{-1}\ km^{-2}$), i.e., discharge divided by drainage area of the basin.

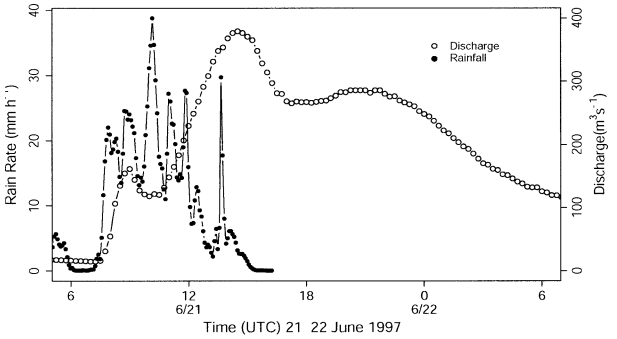

FIG. 3. Basin-averaged rainfall rate and discharge for the Menomonee River at Wauwatosa, 0600 UTC 21 Jun–0600 UTC 22 Jun 1997. Rainfall rate time series are averaged to 15-min time interval.

and management problems, but the regional flood response of urbanizing basins is poorly understood (see Leopold 1968; Graf 1977; Smith et al. 2002). In this study, our objective is to examine the regional flood response of the Menomonee River basin and identify land surface and rainfall properties that are dominant controls of extreme flood response.

Space–time variability of rainfall is examined through analyses of rainfall fields derived from Weather Surveillance Radar–1988 Doppler (WSR-88D) volume scan reflectivity observations. Particular attention is given in section 2 to the contrasting structure, motion, and rainfall rates from the 21 June 1997 and 6 August 1998 storms (for related analyses, see Doswell et al. 1996; Smith et al. 1996, 2001, and 2002; Ogden et al. 2000; Sturdevant-Rees et al. 2001; Zhang et al. 2001). In section 3 these contrasting storm elements are revisited in light of extreme flood response.

2. Hydrometeorology of the 21 June 1997 and 6 August 1998 storms

In this section, we examine the spatial and temporal variability of rainfall for the 21 June 1997 and 6 August 1998 storms in the Milwaukee metropolitan region. Analyses are based on high-resolution (1-km horizontal scale; 5-min timescale) rainfall estimates derived from volume scan WSR-88D reflectivity observations and rain gauge observations from an urban mesonet maintained by the city of Milwaukee. Supplemental analyses utilize Geostationary Operational Environmental Satellite (GOES) IR observations and cloud-to-ground (CG) lightning observations from the National Lightning Detection Network (see Orville and Silver 1997). Particular attention is given to contrasts in storm structure, evolution, and motion between the June 1997 and August 1998 storms.

Radar rainfall estimation is based on a power-law Z–R relationship and bias correction based on rain gauge observations (see Fulton et al. 1998; Baeck and Smith 1998), with the estimation equation formulated as follows:

$$R = BaZ^b, \tag{1}$$

where R is rainfall rate (mm h^{-1}), Z is the radar reflectivity factor ($mm^6\ m^{-3}$), a and b are Z–R parameters, and B is the multiplicative bias. The default WSR-88D Z–R relationship is used with $a = 0.017$ and $b = 0.71$. A 55-dBZ cap is applied to reflectivity observations to mitigate the influence of hail contamination. For the four events analyzed in this study the hail cap did not play a significant role in the rainfall analyses. The multiplicative bias B is estimated for each event as the ratio of total rainfall from the rain gauge network and total rainfall from radar bins containing rain gauges. Rainfall estimates are developed at 1-km horizontal resolution and 5-min timescale.

Flooding in the Menomonee River basin on 21 June 1997 resulted from a series of storms that passed over the basin from 0630 until 1330 UTC. At 0700 UTC (Fig. 4a), a small area of convection was developing between a decaying mesoscale convective system (MCS) centered over Michigan and a large MCS over Iowa (see also Roebber and Eise 2001). The MCS developing over Milwaukee intensified and remained nearly stationary until 1100 UTC (Figs. 4b,c). The western MCS passed over the Milwaukee region at 1300 UTC (Fig. 4d) ending the period of heavy rainfall in the Menomonee River basin.

The large-scale evolution of weather systems on 21 June (Fig. 4) was linked with storm-scale evolution over

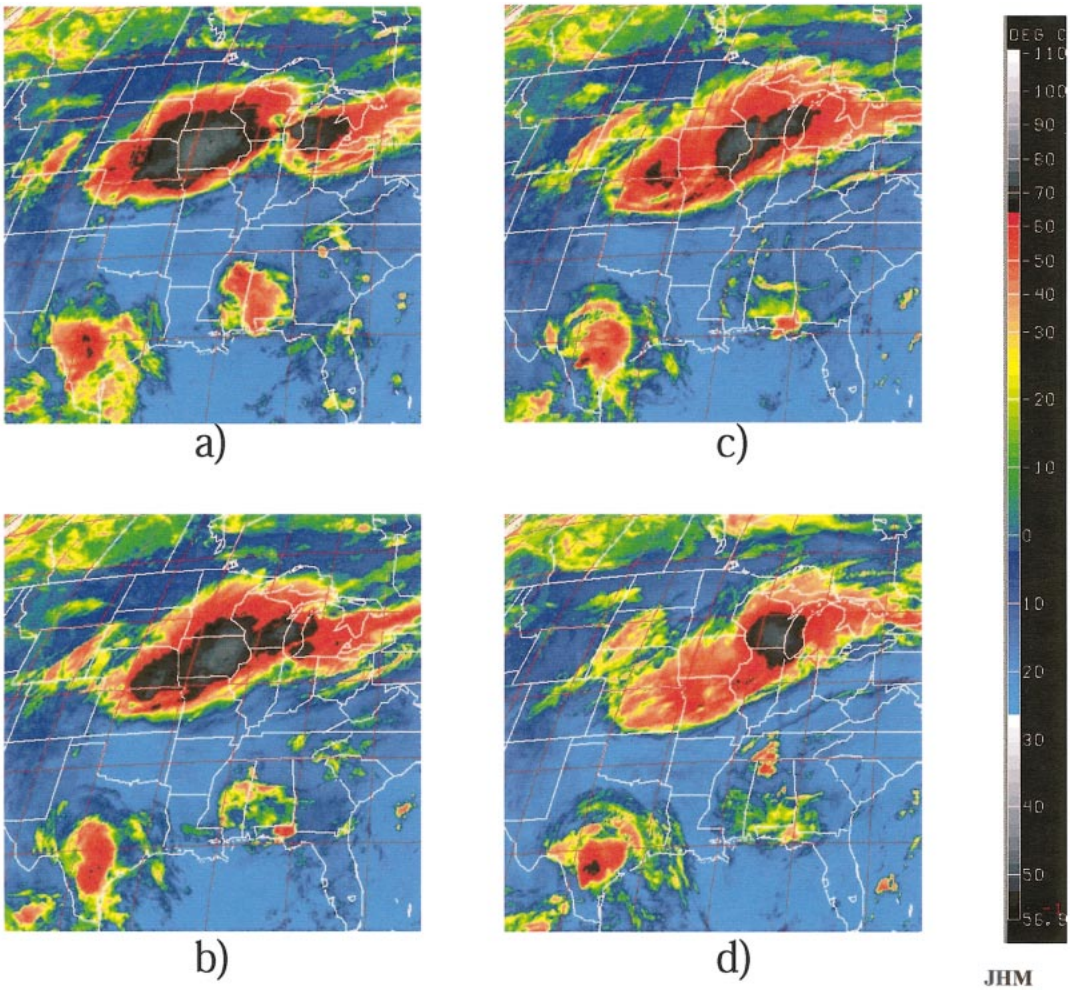

FIG. 4. GOES IR imagary on 21 Jun 1997 at (a) 0700 UTC, (b) 0900 UTC, (c) 1100 UTC, and (d) 1300 UTC.

the Milwaukee region (Fig. 5). At 0717 UTC (Fig. 5a), convective elements were oriented along an east–west boundary. A north–south oriented outflow boundary (apparent in Fig. 5a as a reflectivity *thin line* west of the Menomonee River basin) moving from east to west served as a focusing mechanism for convective development and intensification. Heavy rainfall in the Menomonee River basin was concentrated in the center and lower portion of the basin (Fig. 5a). From this time until the arrival of the western MCS, convective elements tracked repeatedly over the Milwaukee region [see Chappell (1989) for discussion of *quasi-stationary* behavior of storm systems]. Intensification of the Milwaukee MCS (Fig. 5b) resulted in an organized region of convection extending along an east–west axis through the upper half of the Menomonee basin at 0946 UTC. During the decaying phase of the Milwaukee MCS (Fig. 5c; 1126 UTC), a north–south-oriented line of convection covered much of the Menomonee River basin below Menomonee Falls. Passage of the western MCS over the Milwaukee Region (Fig. 4d) was associated with a rapidly moving arc of convection (Fig. 5d). Time lapse imagery of radar reflectivity fields (not shown) illustrate the rotation of the band of convection about the center of the MCS circulation, which at 1310 UTC was located close to the Milwaukee radar.

Gauge–radar intercomparisons for the 21 June 1997 storm (Figs. 6 and 7a and discussion below; rain gauge locations are shown in Fig. 7a) illustrate the capability of radar rainfall estimates to represent the temporal and spatial variability of extreme storm rainfall. The estimated multiplicative bias, B, for the event is 1.11, reflecting an 11% underestimation of rainfall with the default Z–R relationship. The root-mean-square error (rmse) of 15-min rainfall estimates of 11.5 mm h^{-1} is 66% of the mean 15-min rainfall rate (for 15-min periods with positive rainfall rates). The rmse of rainfall rate estimates at 60-min timescale, 5.4 mm h^{-1}, is 42% of the mean 60-min rainfall rate (for hours with positive rainfall). The storm total RMSE of 14.3 mm is 12% of mean storm total rainfall of 103 mm. A significant contribution to rmse, especially at shorter timescales, arises

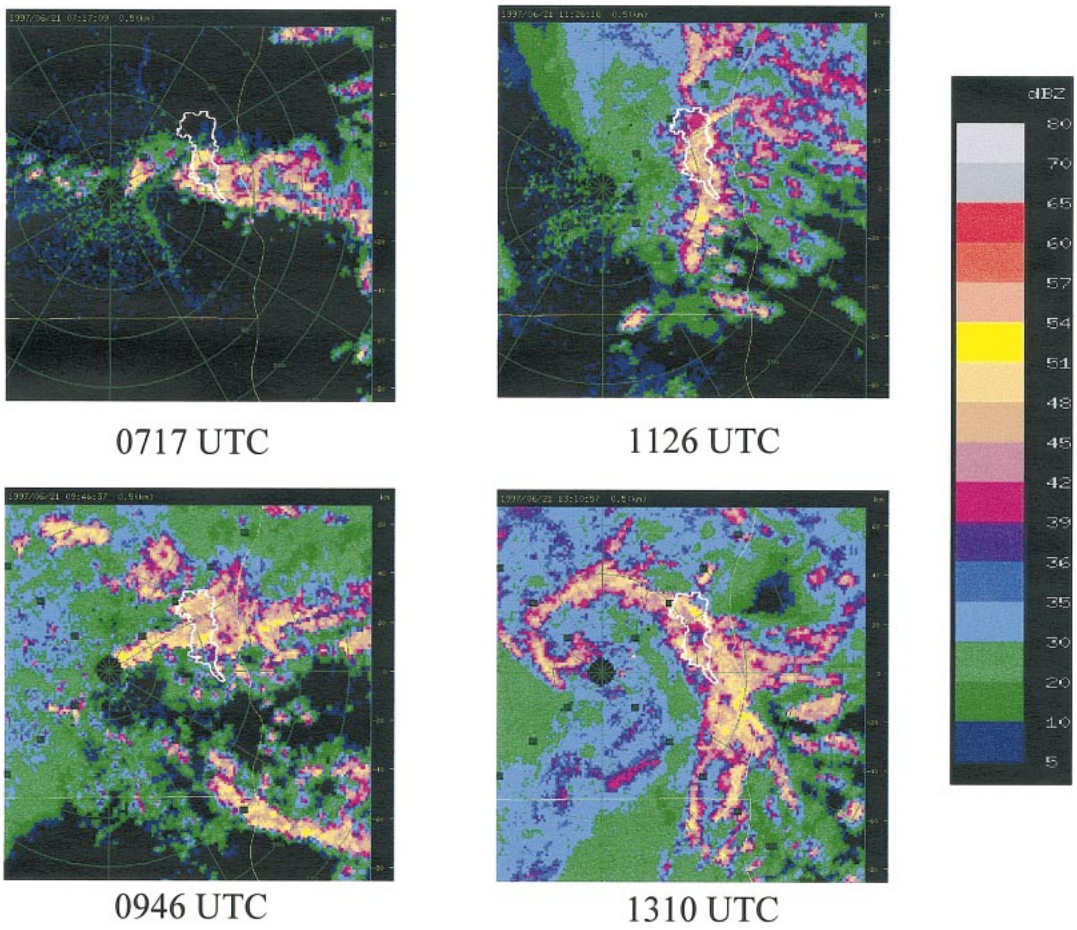

FIG. 5. WSR-88D reflectivity fields on 21 June 1997 at (a) 0717 UTC, (b) 0946 UTC, (c) 1126 UTC, and (d) 1310 UTC.

from the sampling differences between radar and rain gauges (see Ciach and Krajewski 1999; Anagnostou et al. 1999).

The storm total rainfall map (Fig. 7a) for the period 0600–1400 UTC reflects the structure and motion of storm elements over the region [see Chappell (1989) for additional discussion], with an elongated rainfall maximum greater than 100 mm extending from 20 km west of the basin to 30 km east of the basin. The 100-mm contour encloses most of the Menomonee River basin.

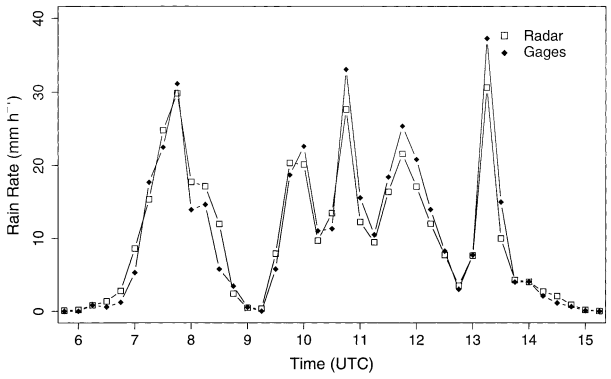

FIG. 6. Time series of radar and rain gauge rainfall estimates at 15-min timescale. Gauge analyses are averaged for 18 rain gauges in Milwaukee urban rain gauge network. Radar analyses are for the 18 1-km bins that contain the rain gauges.

The synoptic-scale environment of the 6 August 1998 storm included a cold front extending from southwest of the Rio Grande River in Mexico to northern Illinois, and a warm front oriented from southwest to northeast through Milwaukee (National Oceanic and Atmospheric Administration Daily Weather Maps; figures not shown). Widespread convection developed ahead of the cold front and wrapped around the upper-level low. The flood-producing storms over the Milwaukee region tracked along the warm front from 1800 to 2400 UTC on August 6. During this period, storms formed southwest of Underwood Creek along the frontal boundary and were steered over Underwood Creek and the center of the Menomonee River basin (Fig. 8).

The storm total rainfall distribution for the 6 August 1998 storm (Fig. 7b) reflects storm structure and motion, as controlled by the frontal boundary and steering winds aloft. Of particular importance for flooding in Under-

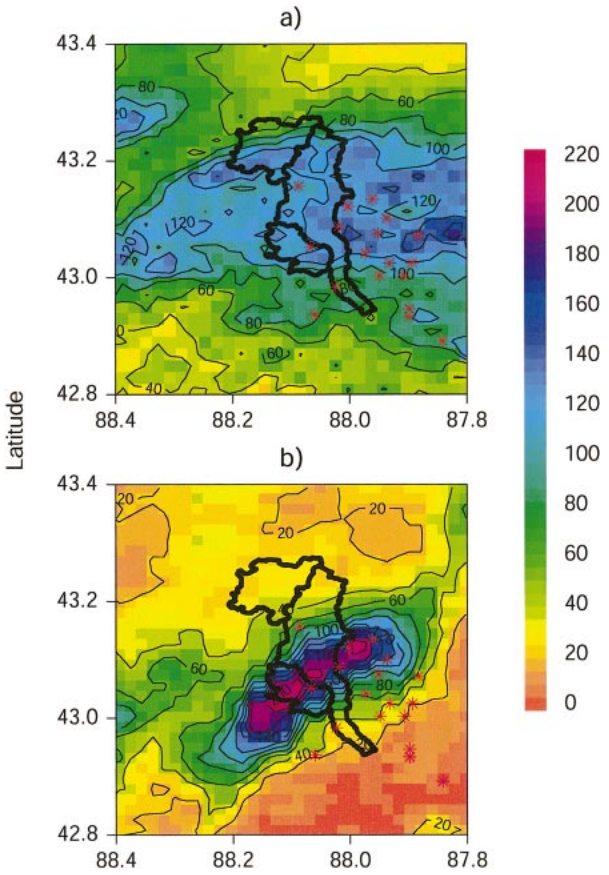

FIG. 7. Storm total rainfall (mm) for (a) 21 Jun 1997 and (b) 6 Aug 1998 storms. Rain gauges are shown as red asterisks.

wood Creek was the 2.5-h period beginning of 2030 UTC (Fig. 8) during which persistent high rainfall rates occurred over Underwood Creek. As with the 21 June 1997 storm, there was good agreement (not shown) between radar rainfall estimates and rain gauge observations. Four rain gauges were located within the 140-mm storm total contour (Fig. 7b). Storm total accumulations for these gauges ranged from 160 to 200 mm.

Scaling analyses of rainfall fields (Figs. 9 and 10) illustrate contrasting temporal evolution and spatial structure of the 21 June 1997 and 6 August 1998 storms [see Perica and Foufoula-Georgiou (1996) and references therein for related analyses]. Analyses were carried out for rainfall fields averaged over length scales of 1, 4, and 16 km. The domain used for scaling analyses is a 128 km by 128 km region centered on the Menomonee River basin. A rainfall threshold of 1 mm h^{-1} was used to distinguish rain–no rain areas at 1-km resolution (results are similar in form over a range of rain-rate thresholds, 0.25–2.5 mm h^{-1}, commonly used for rain–no rain analyses; see Baeck and Smith 1995) Analyses of fractional coverage, mean rainfall (for positive bins), and coefficient of variation (mean divided by standard deviation) of rainfall rate (for positive bins) were performed for rainfall rate fields averaged over the 1-, 4-, and 16-km grids.

Scaling analyses highlight the contrasting temporal evolution of two storms that exhibit ''quasistationary'' (Chappel 1989) behavior. For the June 1997 storm there was a sharp increase in fractional rain area with evolution of the Milwaukee MCS and arrival of the western MCS (Fig. 9). At 0700 UTC, fractional coverage of rainfall was 25% at 1-km resolution, 40% at 4-km resolution, and 70% at 16-km resolution. Fractional coverage increased sharply at 0900 UTC with explosive growth of the Milwaukee MCS (Figs. 4 and 5). By 1300 UTC, fractional coverage was 95% at 16-km resolution, 90% at 4-km resolution, and 70% at 1-km resolution. The 6 August 1998 storm, by contrast, exhibited relatively minor changes in storm properties with time (Fig. 10). Fractional coverage of rainfall for the 6 August 1998 storm increased gradually during the period of peak rainfall. From 1930 to 2300 UTC fractional coverage increased from 10% to 20% at 1-km resolution. The uniform temporal features (and spatial structures; see Fig. 8) of the 6 August 1998 storm are likely due to the role of the frontal boundary in organizing the evolution of convection during the 4-h period of peak rainfall.

There were also contrasts in variability of rainfall rate between the June 1997 and August 1998 storms. For the June 1997 storm, the coefficient of variation of rainfall rate fluctuated around 1.3 for 1- and 4-km analyses and 1.0 for 16-km analyses. For the August 1998 storm, the coefficient of variation fluctuated between 1.5 and 2.0 at all scales from 2000 to 2300 UTC. The August 1998 storm was composed of small cores with high rainfall rates grading to low rainfall rates over short distances. Rainfall rate observations from the Milwaukee rain gauge network at 5-min timescale exceeded 140 mm h^{-1} during the August 1998 storm. Peak rainfall rates from the 21 June 1997 storm were 100 mm h^{-1}.

The storm microphysical and dynamical processes that control the spatial and temporal distribution of extreme rainfall rates are poorly understood, especially at space–time scales relevant to flood production in urban basins, like Underwood Creek. During the period of peak rainfall intensity over Underwood Creek, the August 1998 storm is discernible in GOES IR imagery (figure not shown) only as a small cloud streak with relatively warm cloud-top temperatures (−50°C, as compared with −80°C for the 21 June 1997 storms; see Fig. 4). In this respect, the August 1998 storm is similar to storms like the 28 July 1997 Fort Collins, Colorado, storm in which extreme rainfall rates were linked to efficient warm rain precipitation processes (Petersen et al. 1999; see also Maddox et al. 1978; Smith et al. 1996). Unlike the Fort Collins storm, the August 1998 Milwaukee storm produced large storm total cloud-to-ground lightning flash densities (as did the June 1997 storm; see Fig. 11). For the August 1998 storm, peak flash densities were on the northeast (''downstream'')

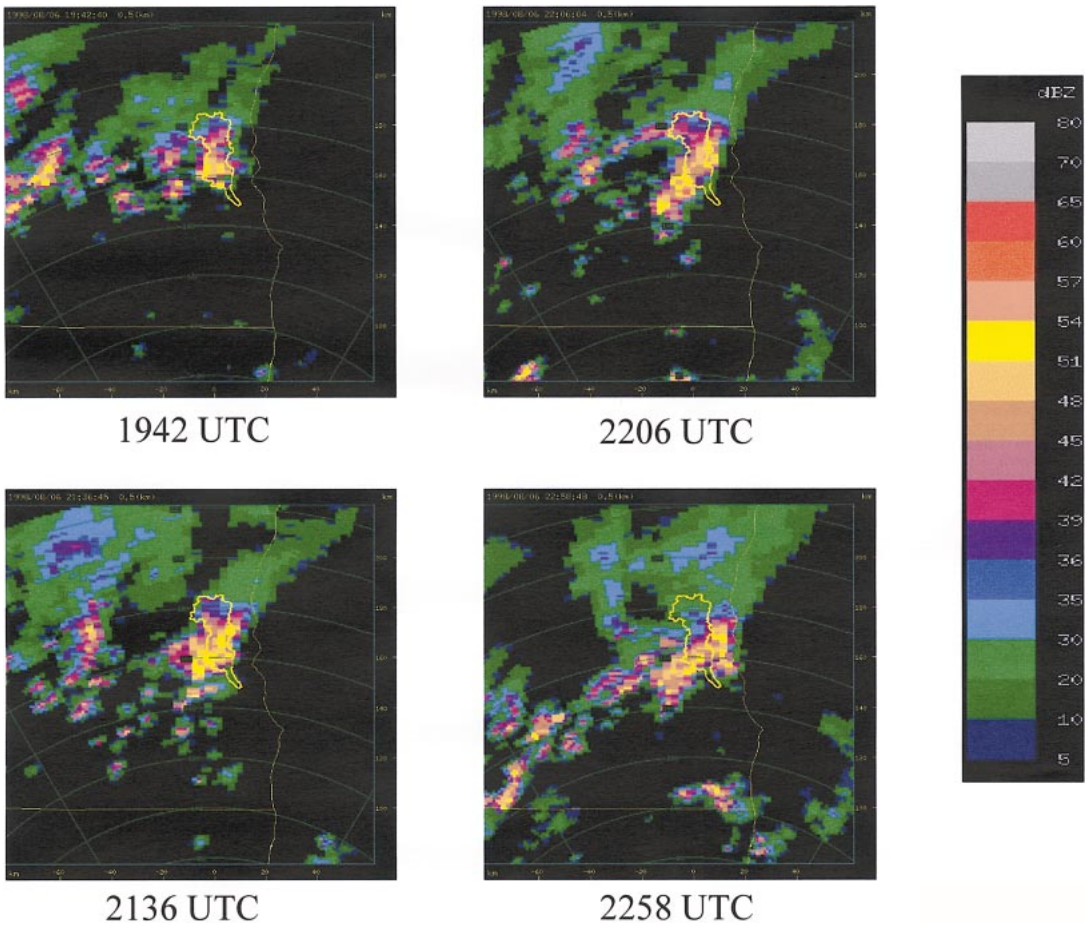

FIG. 8. WSR-88D reflectivity field on 6 Aug 1997 at (a) 1942 UTC, (b) 2136 UTC, (c) 2206 UTC, and (d) 2258 UTC.

end of the region of peak rainfall and followed the period of extreme rainfall production. For the June 1997 storm, peak flash densities were concentrated to the west (''upstream'') of the largest rainfall accumulations (Fig. 11) and preceded production of peak rainfall rates. Advances in understanding microphysical and dynamical processes controlling extreme rainfall rates are needed both for characterizing space–time structure of flood-producing rainfall and for improving remote sensing procedures used for estimating rainfall rate.

3. Flood response of the Menomonee River basin

In this section we examine flood response of the Menomonee River basin with particular emphasis on contrasting response of the lower basin and the upper basin (Fig. 1). Analyses focus on Underwood Creek (in the lower basin) and the Menomonee River above Menomonee Falls (in the upper basin; see Figs. 1 and 2). Land use in the upper basin is dominated by a mix of agricultural and residential regions, with a core of urban development in the lower portion of the basin (Fig. 1). Residential and urban land use categories dominate the Underwood Creek basin. Differences in flood response are examined in terms of the spatial and temporal variability of rainfall forcing. In addition to the 21 June 1997 and 6 August 1998 events, we examine flood response to smaller events on 2 July 1997 and 21–22 July 1999.

The 2 July 1997 storm produced rainfall accumulations ranging from 15 to 40 mm over the Memomonee River basin during the 45-min period beginning 0800 UTC. The storm was a rapidly moving, long-lived thunderstorm system, which produced large hail, damaging winds, and lightning, in addition to extreme rainfall rates over the Milwaukee region. The storm entered the western edge of the Milwaukee WSR-88D area of coverage at 0424 UTC and reached the western margin of the Menomonee River basin at 0754 UTC for an average speed of 71 km h^{-1}. The storm exhibited the hook echo signature of a supercell thunderstorm at the western margin of the radar area of coverage and produced peak reflectivity values between 65 and 70 dB*Z* [compare with the storms described in Smith et al. (2001)]. Reports of damaging winds, large hail, and lightning were concentrated in the area west of the Menomonee River basin. Peak rainfall rates from the Milwaukee rain gauge network exceeded 150 mm h^{-1} at 5-min timescale. At

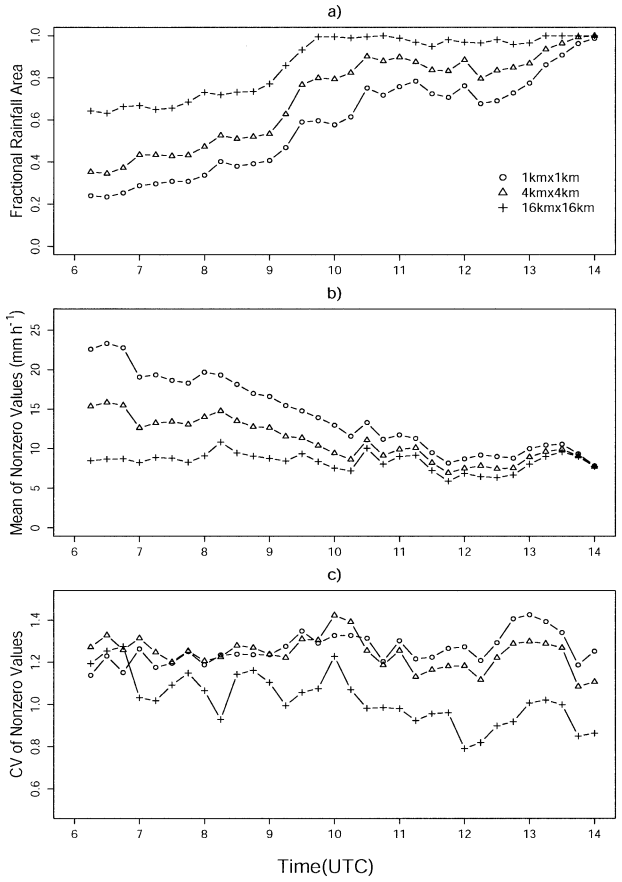

FIG. 9. Time series of (a) fractional coverage ($km^2\ km^{-2}$) of positive rain rates, (b) mean rain rate of nonzero bins, and (c) coefficient of variation of nonzero rain rates on 21 Jun 1997.

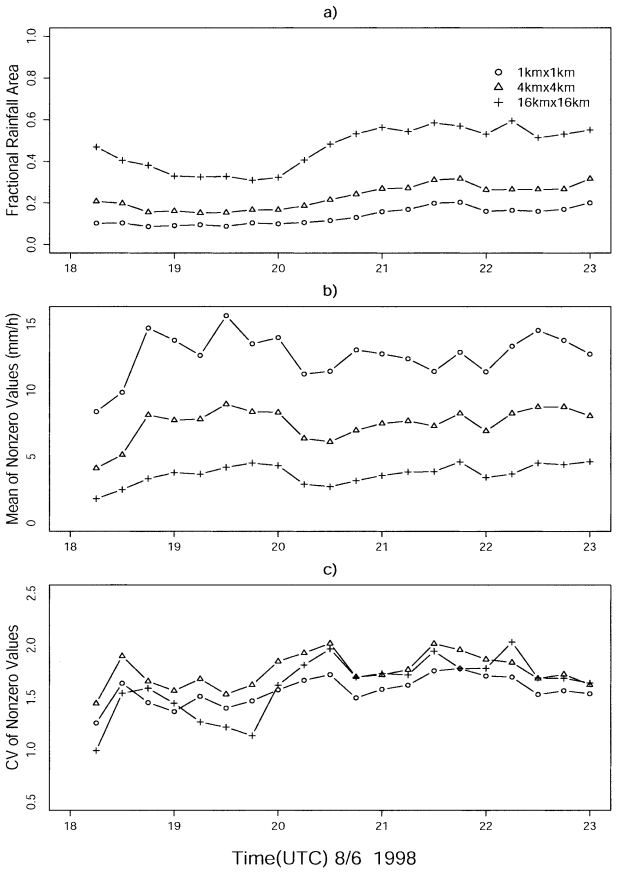

FIG. 10. Time series of (a) fractional coverage of ($km^2\ km^{-2}$) of positive rain rates, (b) mean rain rate of nonzero bins, and (c) coefficient of variation of nonzero rain rates on 6 Aug 1998.

any location within the Menomonee River basin, virtually all of the storm total rainfall was delivered during a time period of less than 20 min. Rainfall accumulations in the Menomonee Falls basin ranged from less than 5 mm in the upper basin to 30 mm near the basin outlet. Rainfall accumulations in Underwood Creek ranged from 20 to 40 mm.

The 21 July 1999 storm was a multicellular thunderstorm that produced rainfall accumulations in the Menomonee River basin ranging from 60 to 110 mm during a 4-h period beginning 0400 UTC. Although the storm produced lightning and there were reports of damaging winds, the most significant impacts of the storm centered on flash flooding throughout southern Wisconsin. Like the 21 June 1997 storm, large rainfall accumulations resulted from multiple storm elements tracking over the region from west to east. Peak rainfall rates from the Milwaukee rain gauge network exceeded 100 mm h^{-1} at 5-min timescale. Rainfall accumulations above Menomonee Falls ranged from 80 to 110 mm. For Underwood Creek, rainfall accumulations ranged from 50 to 80 mm.

Unit Values discharge observations at 15-min time interval from the USGS gauging stations at Menomonee Falls and Underwood Creek were used in conjunction with radar rainfall fields to construct water budgets for the 21 June 1997, 2 July 1997, 6 August 1998, and 21 July 1999 flood events (Tables 1 and 2). Storm total runoff (in mm) was computed by integrating discharge over the duration of the flood and scaling by the basin area.

There are large contrasts in runoff volumes and flood peak magnitudes between Underwood Creek and the Menomonee River above Menomonee Falls (Tables 1 and 2). Runoff ratios for Menomonee Falls range from less than 10% to a maximum of 24%, with little correspondence to rainfall totals. For Underwood Creek, runoff ratio ranged from 30% for low rainfall totals to 70% for the largest rain event. Unit discharge flood peaks ranged from 0.13 $m^3\ s^{-1}\ km^{-2}$ to 0.47 $m^3\ s^{-1}\ km^{-2}$ for Menomonee Falls. For Underwood Creek unit discharge peaks ranged from 1.02 $m^3\ s^{-1}\ km^{-2}$ to 4.20 $m^3\ s^{-1}\ km^{-2}$. The differences in peak unit discharge between Underwood Creek and Menomonee Falls for the four flood events reflect the long-term flood frequency contrasts between the two basins (Fig. 2).

The June 1997 and August 1998 floods in Underwood

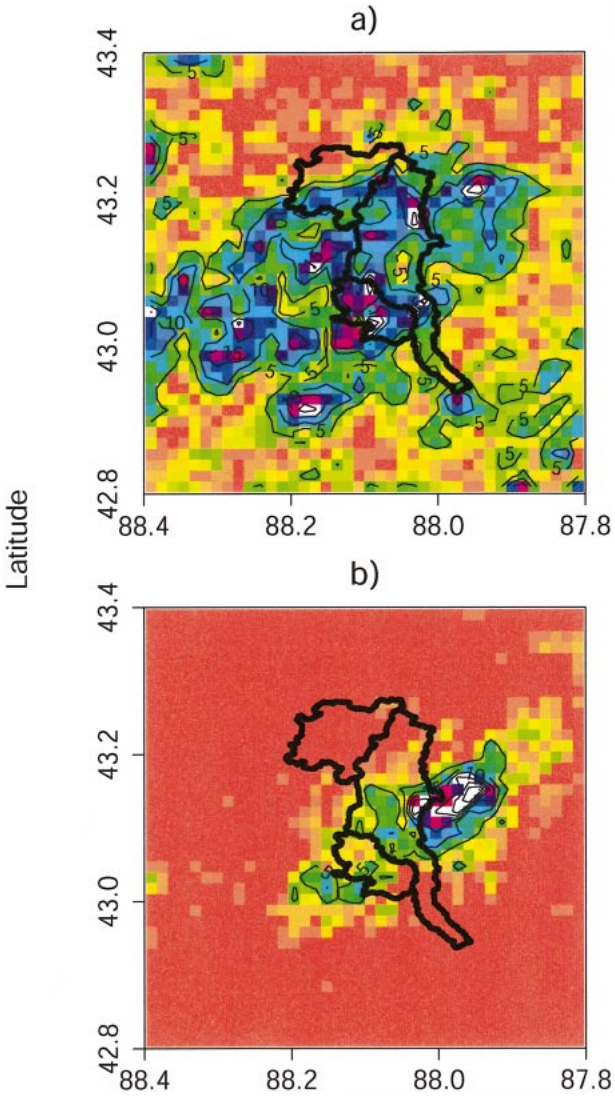

FIG. 11. Storm total cloud-to-ground (CG) lightning strikes (CG strikes km^{-2}) for (a) the 21 Jun 1997 and (b) the 6 Aug 1998 storms. Contours are are 5 CG strikes km^{-2}) interval. Color scale ranges from less than 1 CG strikes km^{-2} (orange), 5–10 CG strikes km^{-2} (green to blue), 10–15 CG strikes km^{-2} (dark blue to purple) and greater than 15 CG strikes km^{-2} (white).

Creek resulted from comparable storm total rainfall accumulations, 131 mm for the June 1997 event and 113 mm for the August 1998 event. The flood peak magnitudes and runoff volumes (Table 2) for the two events, however, were quite different, 62 mm of runoff (runoff ratio of 56%) for the June 1997 event versus 93 mm of runoff (runoff ratio of 70%) for the August 1998 event, and peak discharge values of 130 m^3 s^{-1} for the June 1997 event versus 212 m^3 s^{-1} for the August 1998 event. The August 1998 storm produced higher basin-averaged rainfall rates and a continuous 3-h period (2030–2330 UTC) of heavy rainfall over much of the basin. The June 1997 storm was characterized by multiple pulses of heavy rainfall separated by periods of low rainfall

TABLE 1. Summary of flood events in the Menonomonee River basin above Menomonee Falls.

Event	Total rainfall (mm)	Total runoff (mm)	Runoff ratio	Peak discharge (m^3 s^{-1})	Peak unit discharge (m^3 s^{-1} km^{-2})
21–22 Jun 1997	103	NA	NA	42	0.47
2–3 Jul 1997	18	4.5	0.24	11	0.13
6–7 Aug 1998	28	2.6	0.09	12	0.14
21–22 Jul 1999	96	7.5	0.08	25	0.28

rate (Figs. 5 and 6). The August 1998 storm exhibited larger gradients in storm total rainfall distribution, from 80 mm at the northwest border of the basin to 210 mm in the central core to 80 mm at the southeastern boundary.

A distributed hydrologic model is used to further examine contrasting hydrologic response associated with space–time rainfall variability and heterogeneous land surface properties. The Network Model (Morrison and Smith 2001; Giannoni et al. 2003) combines a grid-based Hortonian infiltration model and network-based hillslope and channel response model. Discharge in the Network Model can be represented as follows:

$$Q(t) = |A|^{-1} \int_A M\left[t - \frac{d_o(x)}{v_0} - \frac{d_1(x)}{v_1}, x\right] dx, \quad (2)$$

where A is the domain of the drainage basin above the specified location, $M(t, x)$ is the runoff rate (mm h^{-1}) at time t and location x ($\in A$), $d_0(x)$ denotes the distance from x to the closest stream channel, and $d_1(x)$ denotes the channel distance from x to the outlet of the basin specified by the region A. The total flow distance from x to the basin outlet is $d_0(x) + d_1(x)$. The drainage network for the Menomonee River basin was extracted from a 30-m Digital Elevation Models data using an area threshold criterion; the aggregate drainage density of the extracted drainage network is 1.7 km km^{-2}. The runoff rate $M(t, x)$ is computed from the rainfall rate $R(t, x)$ (mm h^{-1}) using the Green-Ampt infiltration model with moisture redistribution [see Ogden and Saghafian (1997) for algorithm details]. Runoff is assumed to move over hillslopes at a uniform velocity v_0 and through the channel system at velocity v_1 [see Rodriguez-Iturbe and Rinaldo (1997) for discussion of similar models]. Giannoni et al. (2003) present sensitivity anal-

TABLE 2. Summary of flood events in Underwood Creek.

Event	Total rainfall (mm)	Total runoff (mm)	Runoff ratio	Peak discharge (m^3 s^{-1})	Peak unit discharge (m^3 s^{-1} km^{-2})
21–22 Jun 1997	111	62	0.56	130	2.56
2–3 Jul 1997	33	10	0.30	56	1.10
6–7 Aug 1998	131	93	0.70	212	4.16
21–22 Jul 1999	60	24	0.40	92	1.82

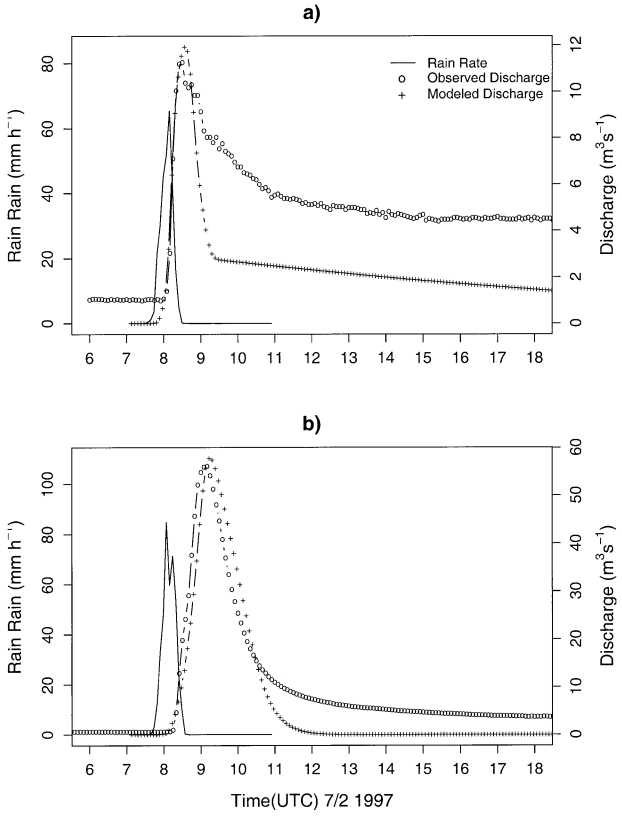

FIG. 12. Modeled and observed hydrographs for (a) Menomonee Falls and (b) Underwood Creek 2 Jul 1997. Solid line represents basin-averaged rain rate.

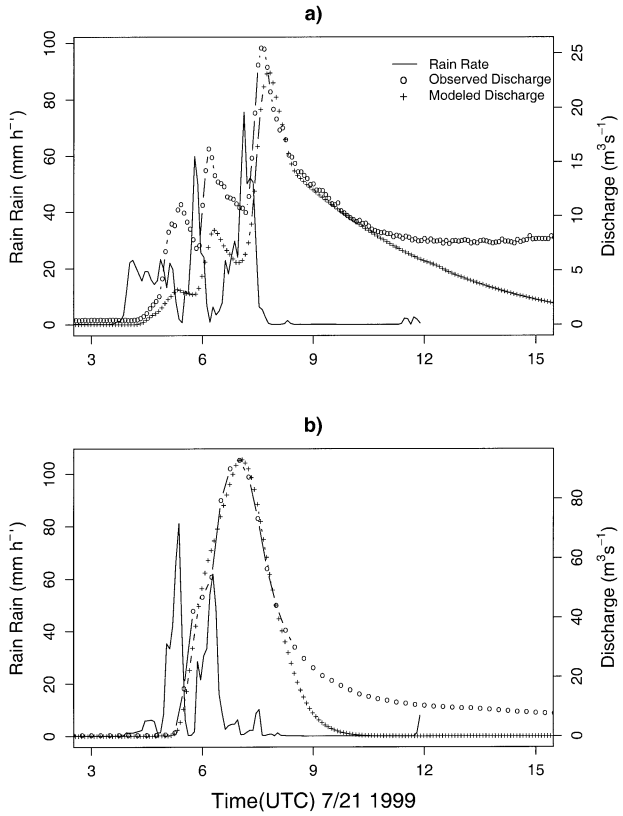

FIG. 13. Modeled and observed hydrographs for (a) Menomonee Falls and (b) Underwood Creek 21–22 Jul 1999. Solid line represents basin-averaged rain rate.

yses of model results to spatial and temporal averaging of rainfall fields.

The 2 July 1997 flood reflects basin response to a unit pulse of rainfall. Model results for Underwood Creek reproduced the flood peak magnitude and timing, as well as the structure of the rising and falling limbs of the hydrograph (Fig. 12b). For Menomonee Falls, it is possible to reproduce the peak magnitude and time to peak, but not the receding portion of the hydrograph (Fig. 12a). The results for Menomonee Falls are consistent with a rapid, Hortonian response in the small, urbanized portion of the basin near the basin outlet (note also water balance analyses in Tables 1 and 2 and discussion below). The slow, attenuated response at Menomonee Falls is due to a combination of non-Hortonian runoff production mechanisms from agricultural and residential portions of the basin and the response of detention basins in the residential areas of the basin.

The July 1999 storm provides a more complex response to several pulses of rainfall in both basins. The Underwood Creek hydrograph can be accurately reproduced but the Menomonee Falls hydrograph cannot (Fig. 13). The model response for Menomonee Falls reproduces the peak discharge and time to peak, but severely underestimates preceding peaks and is unable to capture the falling limb of the hydrograph. The observed hydrograph shows a sharp peak associated with each of the pulses of rainfall. The inability of the model to capture all of the hydrograph peaks is likely due to an inadequate representation of the area producing the peak response.

A notable feature of the Menomonee Falls response is that the lag-to-peak (time difference between peak discharge and time centroid of rainfall) is shorter than for Underwood Creek (recall that the drainage area for Menomonee Falls is 90 km^2; for Underwood Creek the drainage area is 47 km^2). These results support the conclusion presented above that peak response at Menomonee Falls is determined by urbanized portions of the lower watershed (Fig. 1). Runoff production for the remainder of the basin is dominated by non-Hortonian mechanisms and is characterized by a highly attenuated response, relative to the impervious portion of the basin. As noted above, detention basins in areas of residential land use also play a significant role in the attenuated response of the basin. Sensitivity to temporal and spatial variability of rainfall is highest in the small, impervious portion of the Menomonee Falls basin. In regions dominated by non-Hortonian runoff production mechanisms, sensitivity of flood response to spatial and temporal variability is greatly reduced. Storm total rainfall plays a

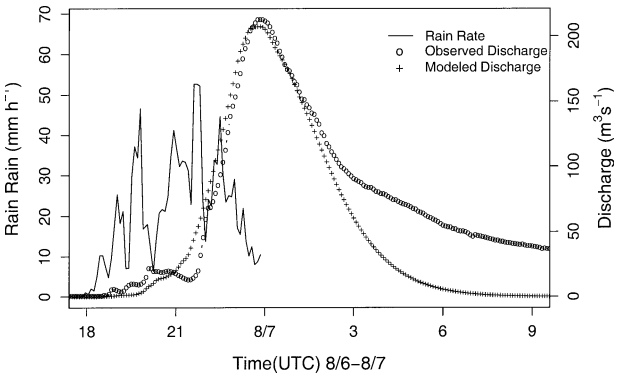

FIG. 14. Modeled and observed hydrographs for Underwood Creek 6–7 Aug 1998. Solid line represents basin-averaged rain rate.

far greater role in determining flood response in these portions of the basin.

For Underwood Creek, the contrasts in flood response between the June 1997 and August 1998 storms are tied to spatial and temporal variability of rainfall rate over the basin, and not basin-averaged storm total rainfall. Structure and motion of the August 1998 storms resulted in a single peak hydrograph (Fig. 14), in which the principal storm elements contributed to peak response [see Smith et al. (2000, 2001, and 2002) and Sturdevant-Rees et al. (2001) for additional discussion of the role of storm structure and motion for extreme flood response].

Flood response in the Menomonee River basin to the 21 June 1997 storm (see Fig. 3) represents a complex interplay of space–time rainfall variability and heterogeneous land surface response. The multipeak structure of the flood hydrograph reflects the quasistationary organization of storm elements and contrasts in runoff production mechanisms over the basin. The peak discharge is primarily associated with Hortonian runoff production in the lower, urbanized portion of the watershed. The final peak, which is characteristic in timing and structure of flood response for other events, results from non-Hortonian mechanisms in the upper basin. Heterogeneous land surface response accentuates the role of space–time variability of rainfall for extreme flood response.

4. Summary and observations

The 21 June 1997 and 6 August 1998 storms were organized systems of thunderstorms that produced record flooding in the Menomonee River basin and its tributaries. The storms exhibited contrasts in structure, motion, and magnitudes of rainfall rates. Scaling analyses based on 1 km, 5-min radar rainfall fields illustrate the contrasting structure and evolution of rainfall for the two events.

Contrasting storm properties between the June 1997 and August 1998 storms resulted in differences in extreme flood response, especially in the most urbanized area of the Menomonee River basin. Although storm total rainfall in Underwood Creek ranged only from 111 to 131 mm for the events, timing and magnitude of flood peaks differed markedly for the events. The mode of convective organization plays an important role in flood response, especially for small urban watersheds. Microphysical controls of extreme rainfall rates from convective systems also play an important role in extreme flood response of small urban watersheds.

There are large contrasts in flood response in the Menomonee River basin between regions of contrasting land use and cover. Unit discharge flood peaks in Underwood Creek are 5–10 times larger than those in the upper basin. Flood response for the upper basin is characterized by a fast-responding peak, which is generated from a small impervious region close to the basin outlet. For the Menomonee River above Menomonee Falls runoff processes controlling flood peaks are largely decoupled from processes controlling flood volume. Regional flood response of the Menomonee River basin to extreme rainfall is strongly dependent on both space–time variability of rainfall rate and heterogeneities of runoff production.

Acknowledgments. This research was funded in part by the U.S. Army Research Office (Grant No. DAAD19-99-1-0163), NASA (NAG5-7544), the National Science Foundation (EAR99-09696 and EAR-0208269), and the National Weather Service. This support is gratefully acknowledged.

REFERENCES

Anagnostou, E. N., W. F. Krajewski, and J. A. Smith, 1999: Uncertainty quantification of mean-areal radar-rainfall estimates. *J. Atmos. Oceanic Technol.,* **16,** 206–215.

Baeck, M. L., and J. A. Smith, 1995: Climatological analysis of manually digitized radar data for the United States east of the Rocky Mountains. *Water Resour. Res.,* **31,** 3033–3049.

——, and ——, 1998: Estimation of heavy rainfall by the WSR-88D. *Wea. Forecasting,* **13,** 416–436.

Chappell, C., 1989: Quasistationary convective events. *Mesoscale Meteorology and Forecasting,* P. Ray, Ed., Amer. Meteor. Soc., 289–310.

Ciach, J. G., and W. F. Krajewski, 1999: On the estimation of radar rainfall error variance. *Adv. Water Resour.,* **22,** 585–595.

Doswell, C. A., III, H. E. Brooks, and R. A. Maddox, 1996: Flash flood forecasting: An ingredients-based methodology. *Wea. Forecasting,* **11,** 560–581.

Fulton, R. A., J. P. Breidenbach, D.-J. Seo, D. A. Miller, and T. O'Bannon, 1998: The WSR-88D rainfall algorithm. *Wea. Forecasting,* **13,** 377–395.

Giannoni, F., J. A. Smith, Z. Zhang, and G. Roth, 2003: Hydrologic modeling of extreme floods using radar rainfall observations. *Adv. Water Resour.,* **26,** 195–203.

Graf, W. L., 1977: Network characteristics in suburbanizing streams. *Water Resour. Res.,* **13,** 459–463.

Leopold, L. B., 1968: Hydrology for urban land planning—A guidebook on the hydrologic effects of urban land use. U.S. Geological Survey Circular 554, 18 pp.

Maddox, R. A., L. R. Hoxit, C. F. Chappell, and F. Caracena, 1978: Comparison of meteorological aspects of the Big Thompson and Rapid City flash floods. *Mon. Wea. Rev.,* **106,** 375–389.

Morrison, J. E., and J. A. Smith, 2001: Scaling properties of flood peaks. *Extremes,* **4,** 5–22.

Ogden, F. L., and B. Saghafian, 1997: Green and Ampt infiltration with redistribution. *J. Irrig. Drain. Eng.,* **123,** 386–393.

——, H. O. Sharif, S. U. S. Senarath, J. A. Smith, M. L. Baeck, and J. R. Richardson, 2000: Hydrologic analysis of the Fort Collins, Colorado, flash flood of 1997. *J. Hydrol.,* **228,** 82–100.

Orville, R. E., and A. C. Silver, 1997: Lightning ground flash density in the contiguous United States, 1992–1995. *Mon. Wea. Rev.,* **125,** 631–638.

Perica, S., and E. Foufoula-Georgiou, 1996: Linking of scaling and thermodynamic parameters of rainfall. *J. Geophys. Res.,* **101** (D3), 7431–7448.

Petersen, W. A., and Coauthors, 1999: Mesoscale and radar observations of the Fort Collins flash flood of 28 July 1997. *Bull. Amer. Meteor. Soc.,* **80,** 191–216.

Potter, K. W., 1991: Hydrological impacts of changing land management practice in a moderate-sized agricultural catchment. *Water Resour. Res.,* **27,** 845–855.

Rodriguez-Iturbe, I., and A. Rinaldo, 1997: *Fractal River Basins.* Cambridge University Press, 547 pp.

Roebber, P. J., and J. Eise, 2001: The 21 June 1997 flood: Storm-scale simulations and implications for operational forecasting. *Wea. Forecasting,* **16,** 197–218.

Smith, J. A., M. L. Baeck, M. Steiner, and A. J. Miller, 1996: Catastrophic rainfall from an upslope thunderstorm in the Central Appalachians: The Rapidan Storm of June 27, 1995. *Water Resour. Res.,* **32,** 3099–3113.

——, ——, J. E. Morrison, and P. Sturdevant-Rees, 2000: Catastrophic rainfall and flooding in Texas. *J. Hydrometeor.,* **1,** 5–25.

——, ——, Y. Zhang, and C. A. Doswell III, 2001: Extreme rainfall and flooding from supercell thunderstorms. *J. Hydrometeor.,* **2,** 469–489.

——, ——, P. Sturdevant-Rees, J. E. Morrison, D. Turner-Gillespie, and P. Bates, 2002: The regional hydrology of extreme floods in an urbanizing drainage basin. *J. Hydrometeor.,* **3,** 267–282.

Sturdevant-Rees, P. L., J. A. Smith, J. Morrison, and M. L. Baeck, 2001: Tropical storms and the flood hydrology of the Central Appalachians. *Water Resour. Res.,* **37,** 2143–2168.

Vieux, B. E., and P. B. Bedient, 1998: Estimation of rainfall for flood prediction from WSR-88D reflectivity: A case study, 17–18 October 1994. *Wea. Forecasting,* **13,** 407–415.

Zhang, Y., J. A. Smith, and M. L. Baeck, 2001: The hydrology and hydrometeorology of extreme floods in the Great Plains of eastern Nebraska. *Adv. Water Resour.,* **24,** 1037–1050.